Bull. Mater. Sci., Vol. 7, Nos 3 & 4, October 1985, pp. 341–352. © Printed in India.

Neutron scattering from fractals

S K SINHA

Corporate Research Science Laboratories, Exxon Research and Engineering Company, Route 22 East, Annandale, New Jersey 08801, USA

Abstract. We describe briefly the concept of fractal dimension as applied to both mathematical and statistical fractals. We then discuss the scattering of radiation from fractals and describe the results of small angle neutron scattering studies of the aggregation of small particles in fractal clusters.

Keywords. Fractals; fractal dimension; small angle neutron scattering aggregates.

1. Introduction

The concept of "fractal dimension", which has been gaining increasing attention in condensed matter physics over the last few years, originates in a purely mathematical sense from the study of certain geometrical objects, and has actually been around for quite some time (Hausdorff 1919). The modern formulation of this concept, the further development of this subject and also the term "fractal" is due to the work of Mandelbrodt (1983). In this introduction, I shall attempt to give a *physical* feeling for the concept of an object which has a non-integral dimension. If one considers a stretched string, it is clearly a one-dimensional object (at least beyond a length equal to the thickness of the string). On the other hand, if one imagines this string placed on a surface and looped back and forth so that it begins to almost cover the surface completely, it begins to look like a *two-dimensional* object, and if one imagines it folded up in a tight ball, it begins to look *three-dimensional.* Since this is a continuous process, and there will in general always be holes (i.e. the object may not be completely space filling) at a particular stage, one can then say that the *dimensionality* of the object evolves continuously from 1 to 3. Similarly, a sheet of paper is clearly a two-dimensional object, but if it is crumpled continuously onto itself until it is a tight wad of paper, it begins to approach being three-dimensional. While the above argument is intuitive in understanding, for instance, what one means by an object having a "fractal dimension" of 2·5, it is not enough to define the concept of a fractal object. It is necessary to introduce the concept of *self-similarity* or *scale invariance.* This is really a symmetry property (dilation symmetry) and states that a *portion* of the object, when suitably scale expanded, is indistinguishable from the whole object. For the so-called "geometrical fractals" formed by mathematical construction, this scale invariance is generally valid for discrete scale factors, such as the Koch curve illustrated in figure 1. This curve is generated by taking a straight line, and replacing it by a zig-zag made up of three equal segments each equal in length to half that of the original line, and then continuing to iterate this process. Segments of this curve, blown up by suitable factors of two in length

STAGE	R	n
0	l	1
1	$2l$	3
2	$4l$	9
3	$8l$	27
K	$2^K l$	3^K

$$K = \log_3 n = \log_2 (R/l)$$

$$\therefore\ n = (R/l)^{\ln 3/\ln 2}$$

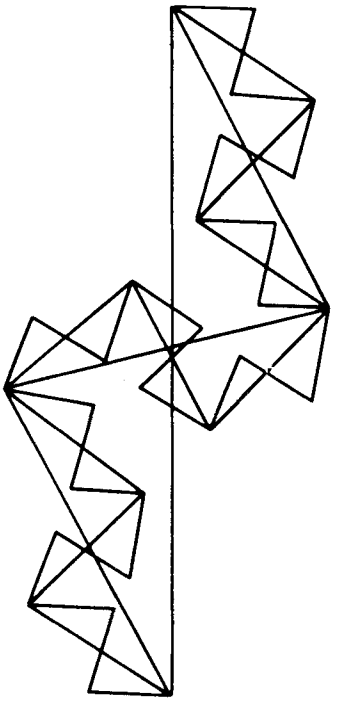

Figure 1. A variation of a Koch curve as an example of a mathematical fractal. The length-radius relationship implies a fractal dimension $D = (\ln 3/\ln 2)$.

scale and suitable rotated, will fit exactly on the original curve. Also the zig-zag nature (down to ever smaller length scales) causes a blurring of the original curve so that it reaches a dimension greater than 1, but not quite 2 (it is not completely space-filling). Another classic example is the Sierpinski gasket (Sierpinski 1979). On the other hand, physical realizations of fractals occurring in Nature possess the symmetry property of self-similarity only in a *statistical sense*. For example, a random spatial distribution of circles on a plane, or spheres in three-dimensions with a *power-law* size distribution [$N(a) \sim a^{-\alpha}$, where a is the radius] possesses the property of scale invariance for all length scale changes.

This property of *geometrical scaling*, when recognized, brings a remarkable symmetry property out in apparently complex and quite disordered systems, and as in the case of Bloch's theorem for periodic symmetries, results in a mathematical relationship involving the structure of the object, as follows: Let $N(r)$ be the number of particles (or equivalently some measure of the mass) within a radius r of a chosen origin. The symmetry with respect to scale changes or *dilation symmetry* implies that

$$N(\lambda r) = \lambda^D N(r) \tag{1}$$

where λ, D are arbitrary constants. Choosing $\lambda = 1/r$ yields

$$N(r) \propto r^D \tag{2}$$

i.e. we have a scaling law for the mass of the object as a function of the radius r. $D = 1, 2, 3$ will easily be recognized as special cases characteristic of familiar 1, 2

and 3-dimensional objects, respectively. However, (2) admits of *arbitrary* values of the exponent D and may be taken as the fundamental equation defining the *fractal dimension* D. (Obviously $D > 3$ cannot be realized in our ordinary embedding three-dimensional space.) The above definition applies to so-called *bulk fractals*. In the case where $N(r)$ denotes the measure of the total *surface area* within a radius r of some point on the surface of an object (such a radius being defined in three dimensions), (2) serves to define the *surface fractal dimension* D_s, which must have a value between 2 and 3.

If (2) holds in a statistical sense around *any* point on an object (which thus must be assumed to be infinite), then it immediately leads, by differentiation, to an expression for the pair-correlation function $g(r)$, defined as the probability density of finding a particle at r, given another particle at the origin. The result is

$$g(r) = A/r^{d-D} \tag{3}$$

where A is a constant and d the dimension of the embedding space. Since the scattering function for beams of neutrons or x-rays, i.e. the structure factor $S(q)$ is given by the Fourier transform of $g(r)$, we have

$$S(q) \sim q^{-D} \tag{4}$$

where q is the neutron or x-ray wavevector transfer. Equation (4) shows that the scattering from a fractal object is of a form similar to that known for critical scattering at the critical point (a special case where we do in fact have dilation symmetry, as well-known from the theory of critical phenomena), and is the starting point for our contention that the fractal nature of certain physical systems can indeed be confirmed by scattering experiments, and the fractal dimension determined. Incidentally, (4) can be easily physically understood as follows: Diffraction experiments probe the density correlations on length scales which correspond to the inverse wavevector transfer q^{-1}, and since the scattered intensity per particle scales with the correlated mass in the probing volume, by (2), it is expected that the intensity scales as q^{-D}. However, as will be discussed later, in real physical systems, the scale invariance is limited to a finite range between upper and lower bounds and this will modify the scattering function.

In this paper, we shall concentrate mainly on small-angle scattering experiments carried out on aggregation of silica particles and gold colloid particles. The clustering of small particles into large ramified objects is a commonly occurring phenomena. In biological systems one finds protein-aggregations, in colloid and polymer chemistry one finds coagulation, flocculation and gel formation and in metallurgy one finds a range of nucleation and growth processes all of which can be treated theoretically in terms of kinetic models of the kind first discussed by von Smoluchowski (1916).

Recent efforts in this field have been stimulated by the observation that the resulting clusters often show a considerable, and quite remarkable, degree of self-similarity or scale-invariance. Especially, the work by Forest and Witten (1979) on silica smoke-particles and the subsequent computer simulations by Witten and Sander (1981, 1983), who devised the simple, elegant diffusion limited aggregation (DLA) model, have started an avalanche of both experimental and theoretical work which seeks a quantitative understanding of aggregation processes. Figure 2 illustrates a computer simulation of a DLA aggregate in $2D$ grown according to the rules of the DLA process (1981, 1983).

The first set of experiments relates to small-angle neutron scattering from low density powders of silica smoke particles which are available commercially under the trade

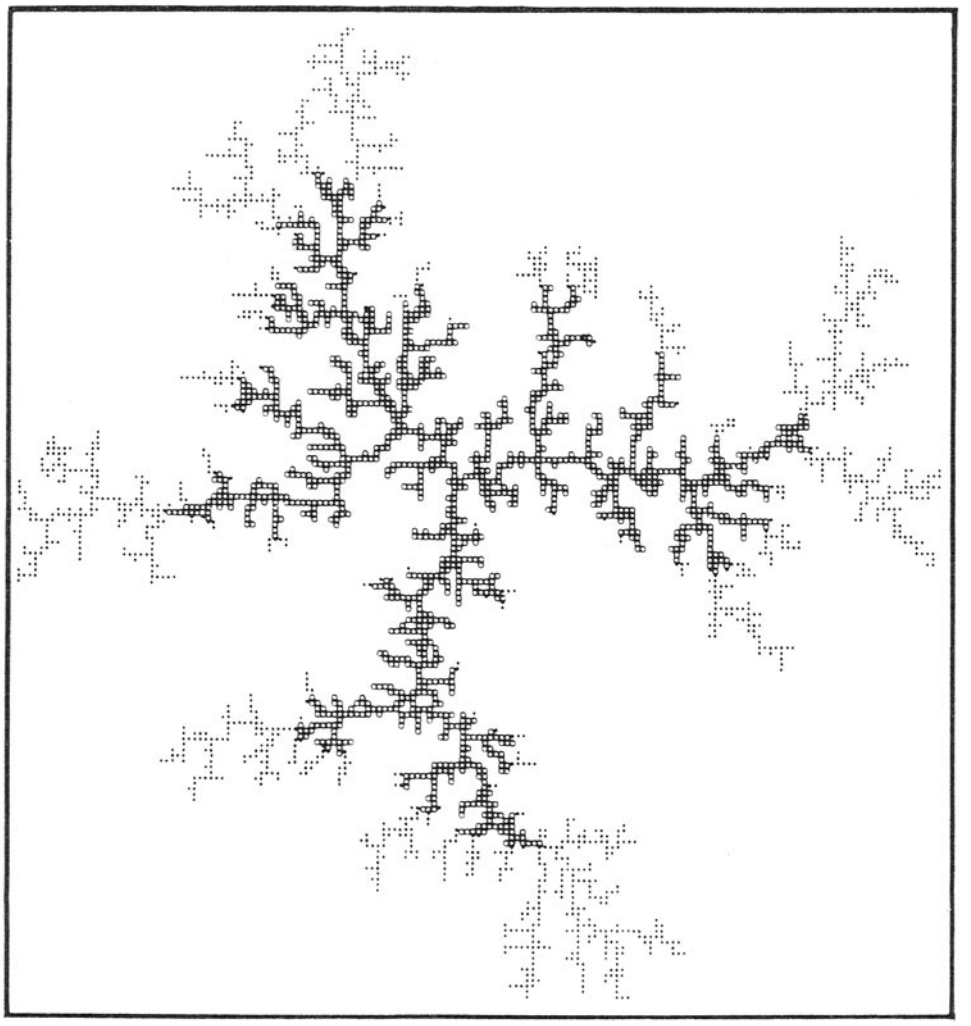

Figure 2. Computer simulation of a DLA aggregate cluster in 2 dimensions (from Sander 1984).

names Cab-O-Sil and Alfasil*. They are produced by the process of flame hydrolysis, in which $SiCl_4$ is burned to give a snow-like product in which the basic small particle units are amorphous SiO_2 spheres of roughly 5 nm diameter. The process of colloidal aggregation has also been studied by Weitz *et al* (1983, 1984) who used electron microscopy to characterize the geometry and in this paper we show how their values for D are confirmed by diffraction experiments using light, x-ray and neutron scattering.

* Cab-O-Sil (grade M5) is a trademark of the Cabot Corporation. Alfasil sample was stock no. D89376 (Alfa Catalog 1981).

2. Experimental details and results for silica aggregates

For the silica particle aggregates, three sets of samples were prepared for the present experiments based on commercially available material. Samples with densities ranging from 0·05 g/cm^3 to 0·2 g/cm^3 were made by packing the materials in 1 and 2 mm thick cuvettes. Samples with densities up to 0·5 g/cm^3 were made by pressing equal amounts of material into 20 mm discs using a hydraulic press. Note that the highest density studied was still much lower than that of bulk silica ($\sim$ 2·5 g/cm^3). Suspended samples were prepared by mixing 2% Cab-O-Sil with water of different H_2O/D_2O ratios and decanting the liquid after centrifugation, yielding low concentrations of the aggregates ($\sim$ 0·006–0·008 g/cm). Samples with different contrasts (H_2O/D_2O ratio) were investigated to ensure that aggregates were entirely dispersed, i.e. that no enclosed air remained in closed pores giving rise to additional scattering.

The experiments were carried out at the SANS facility (Kjems 1985) at the RISØ reactor in Denmark, using a mechanical velocity selector ($\Delta\lambda/\lambda \sim 0{\cdot}18$) for monochromation of the beam, and an area detector. Measurements were made at neutron wavelengths of 6 Å and 22 Å and the two sets of data with overlapping q-ranges were properly normalized to each other to obtain $S(q)$ between 0·008 Å^{-1} and 0·08 Å^{-1}. The area detector efficiency was normalized by carrying out scattering from a 1 mm H_2O sample at both wavelength configurations.

Figure 3 shows a double-log representation of the radial averaged scattering curves

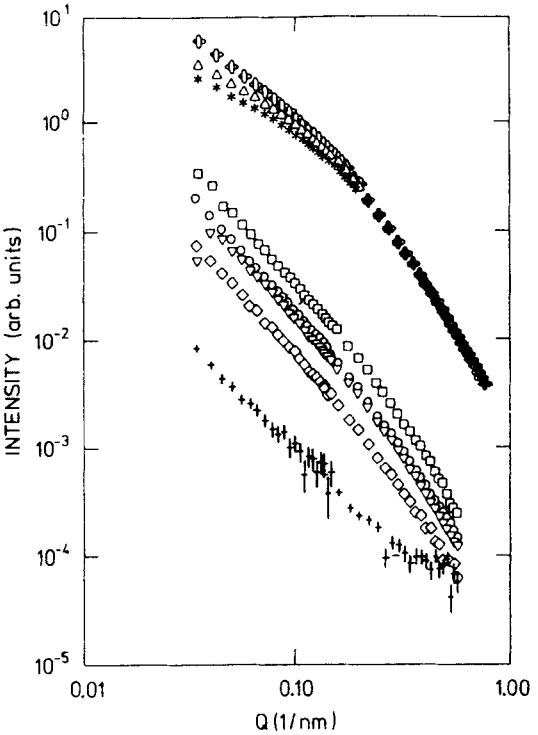

Figure 3. Log-Log representation of SANS scattering curves for aggregated silica samples. The data are shown in original form corrected only for background and detector efficiency. The upper four curves are the compressed solid samples referred to in the text, while the lower five curves are from the water-dispersed samples.

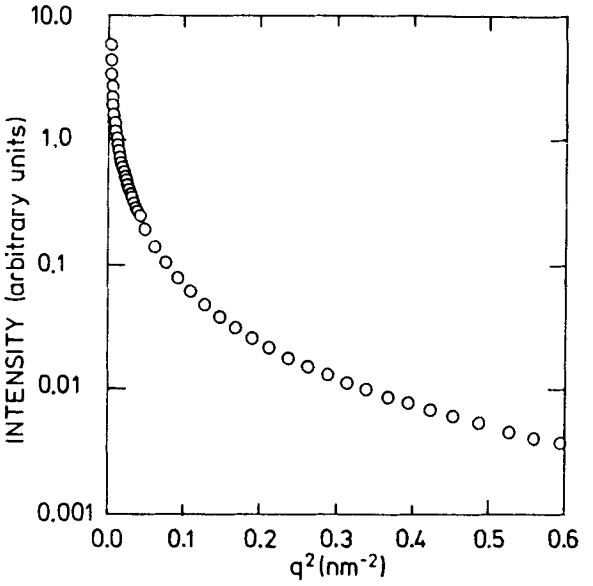

Figure 4. Guinier plot ($\log I$ vs q^2) for a representative sample. As may be seen, no simple characteristic length scale can be deduced from the data.

for the 4 dry samples (F1-F5) with increasing densities and the H_2O/D_2O dispersed samples with roughly the same density. The scattering curves have the same overall shape. The slope increases at higher q and decreases at lower q, the latter being the only region where a significant density dependence was found. Qualitatively, the observed lineshapes conform with the intuitive guess that the low q data ($q\xi \ll 1$, where ξ is a typical cluster size) should show a trend toward saturation due to finite aggregate size.

A representation of the data in a Guinier plot [$\log(I)$ vs. q^2] as shown for a typical sample in figure 4 clearly indicates that there is no simple characteristic length scale to be deduced from the data, except possibly the Guinier radius corresponding to the limiting slope at small q. Scattering curves of this kind are often analyzed as scattering from a hypothetical distribution of spherical particles with a distribution of radii (Schmidt 1982). This approach can be used to represent the present data for the dry samples, but the parameters derived in this fashion do not have any obvious microscopic significance, e.g. the obtained particle size averages show a very strong dependence on density, and yield a narrow distribution of relatively small particles, whose peak occurs at ($\sim$ 30 nm) for the highest densities and a broader distribution of larger particles for the uncompressed samples. This picture is not in agreement with electron micrographs taken from the samples.

We argue that a more natural interpretation of the scattering curves can be based on the assumption of powerlaw correlations between the centers of small fairly monodisperse spherical units ($R \simeq 20$ Å). As shown below, this gives a consistent description of the data at all densities.

As discussed qualitatively in the introduction, the assumption of scale invariance implies the simple but important powerlaw form $I(q) \propto q^{-D}$ for the scattering function. In real systems of aggregates, the scale invariance is limited both at large r (by the finite size of the cluster, or by the entanglement of the clusters) and at small r by the finite size

of the particles making up the aggregate. We now discuss refinements for calculation of $S(q)$, over that represented by (3) and (4). We may write $g(r)$ as

$$g(r) = \delta(r) + g_d(r), \tag{5}$$

where $g(r)$ now represents the pair-correlation function for the *centres* of the spherical particles. For $g_d(r)$ we choose the form

$$\begin{aligned} g_d(r) &= 0 && r < 2r_0 \\ &= (A/r^{d-D})e^{-r/\xi} && r > 2r_0 \end{aligned} \tag{6}$$

representing the effects of both the lower and upper length scale cut-offs. Equation (6) represents the fact that the particle centers cannot approach *closer* than a particle diameter ($2r_0$), and also the fact that for the actual systems we are considering, where the aggregates have a finite cluster size, and furthermore the clusters may be quite entangled, we have to weight $g_d(r)$ with the probability that the fractal correlations around a given particle exist for distances $\geqslant r$. We may represent this by a scaling function $F(r/\xi)$ characterized by a single effective cut-off length ξ, and for simplicity we assume an exponential form for this function. [More complicated forms of the scaling function involving exponentials of arbitrary powers of (r/ξ) could be considered, as has been done by Aharony *et al* (1984) for the case of spin correlations on percolating clusters. The advantage of the present form is that it leads itself to an analytic form for $S(q)$ which may be used to fit the data. Further, as we shall see, it leads to internally consistent values of the fitted parameters.]

Fourier transforming this expression, leads to

$$S(q) = 1 + \frac{C(D-1)\xi^D}{(1+q^2\xi^2)^{D/2}} \frac{[1+q^2\xi^2]^{1/2}}{q\xi} \operatorname{Im}\left\{\left[\left(\Gamma(D-1), \frac{2r_0}{\xi_0} 1 - iq\xi\right)\right]\right.$$

$$\left.[\cos(D-1)\operatorname{Arctan}(q\xi) + i\sin(D-1)\operatorname{Arctan}(q\xi)]/(D-1)\right\} \tag{7}$$

Here $\Gamma(\alpha, z)$ is the incomplete gamma function with complex argument (Schafke 1968) defined by the complex integral

$$\Gamma(\alpha, z) \equiv \int_z^\infty w^{\alpha-1}\exp(-w)\,\mathrm{d}w \tag{8}$$

For $q\xi \gg 1$, $S(q)$ will be approximated by $1 + Cq^{-D}$, while for $q\xi \ll 1$, it will saturate at a value proportional to ξ^D.

Finally, we must take into account the finite particle size, which yields a form factor whose square must be multiplied by $S(q)$ to yield the observed scattered intensity as a function of q, i.e.

$$I(q) \propto S(q) f^2(q) \tag{9}$$

where, for spherical monodisperse particles, the form factor may be written as

$$f(q) = 3\left[\frac{\sin(qr_0) - (qr_0)\cos(qr_0)}{(qr_0)^3}\right]. \tag{10}$$

Equations (8)–(10) were used to make least-squares fits to the data, after first folding with the instrumental resolution in the usual manner, and the fitted models shown with

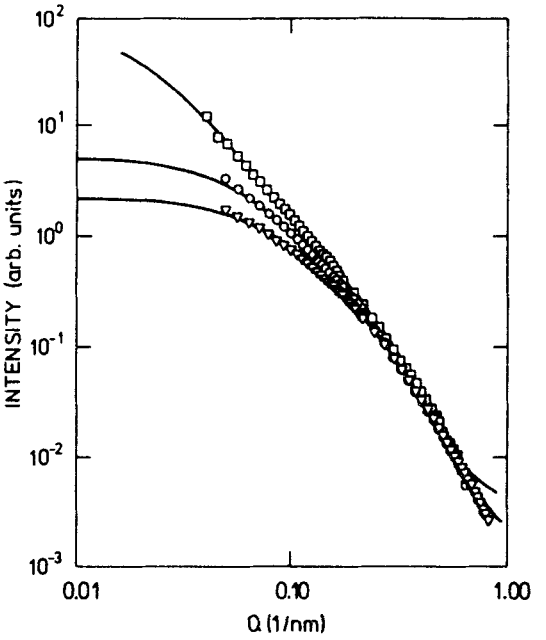

Figure 5. Three representative scattering curves with the fitted model shown (solid curve). Two curves (O and V) are for dry compressed silica aggregate samples, and the third [□] is for a water-dispersed aggregate.

three representative samples in figure 5. From the fits, we conclude that $D = 2{\cdot}6 \pm 0{\cdot}1$ independent of the macroscopic density for the dry samples, while for the dispersed samples $D = 2{\cdot}34 \pm 0{\cdot}1$. The lower value in the latter case may be due to the decanting procedure in the sample preparation or the infused water may cause a slight opening of the structure.

The primary particle radius, r_0, seems to settle around 20 Å for all samples while the upper cut-off, ξ, is systematically related to the macroscopic density, ρ. ξ is found to scale roughly with $\rho^{-1/3}$, as expected if the degree of entanglement of the clusters scales down linearly with the average distance between clusters.

The scale factor A_1, normalized to the number of scatterers, corrected for transmission (and, for the dispersed samples, the contrast), also appears to be fairly constant for all samples. The fluctuations for the dispersed samples are most likely due to inaccuracies in the determination of the SiO_2 concentration in these. This implies that the intensity for $q \to 0$ scales as expected for a fractal syatem $I(q = 0) \propto \xi^D$ [see (8)] giving an independent test of the consistency of the mo-model.

Before concluding the discussion of the silica particle experiments, we note that it is the ability to study the fractal nature of this system over such a wide range of densities that is one of the unique features of our experiment. The experiment thus establishes the usefulness of the concept of an upperlength scale cut-off, ξ, which must be used to analyze scattering data from real (as opposed to mathematical) fractals, as in the case where the aggregated clusters have a finite size or become entangled, thus losing the powerlaw correlations, which exist on a single cluster. The essence of this picture may

thus be applied to systems such as polymer gels or other structures where the powerlaw correlations decay at large length scales.

3. Results for gold colloid aggregates

The gold colloids used in the experiments described here are formed by the reduction of $Na(AuCl_4)$ with sodium citrate (Turkevitch *et al* 1951). They consist of highly uniform spherical gold particles of mean diameter 145 Å and a spread of $\sim 10\%$ in diameter. These particles are initially highly charged and in dilute solution in water and thus do not aggregate. Upon adding a small amount of pyridine, however, the colloidal charge

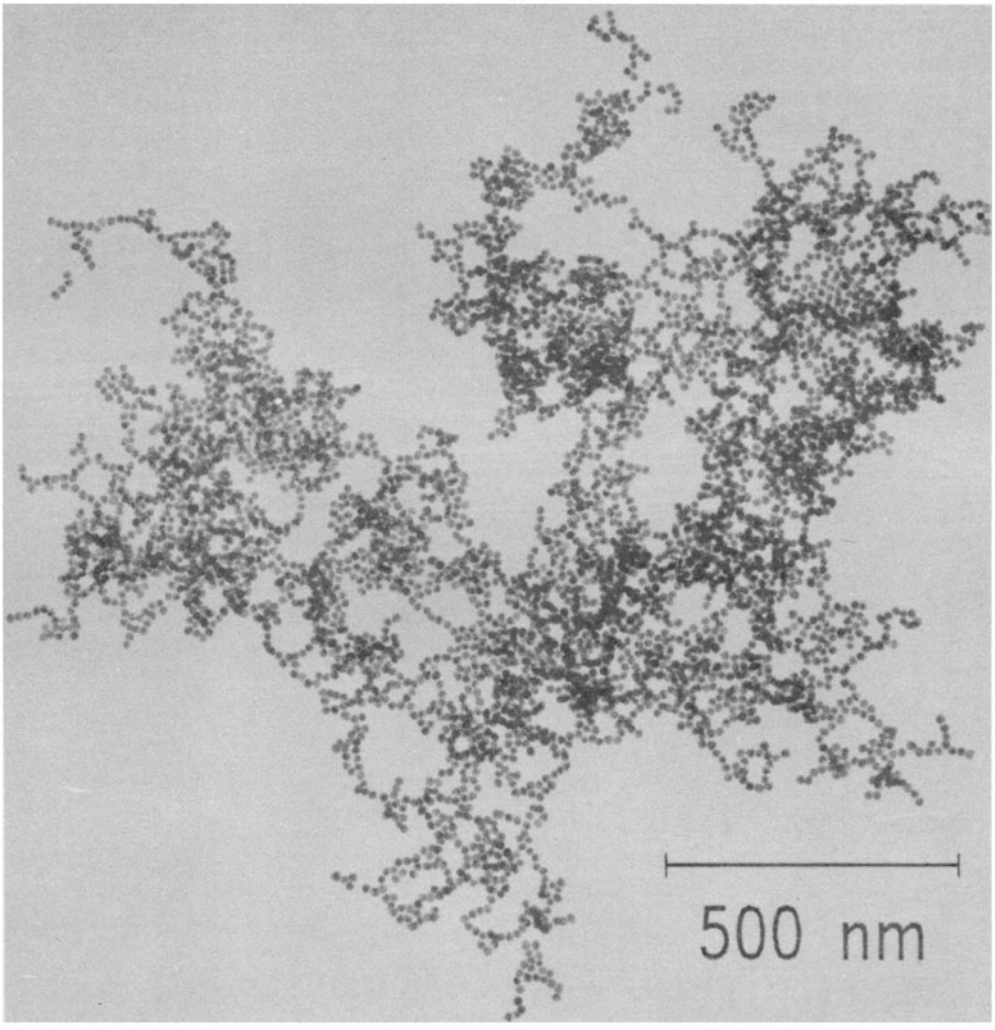

Figure 6. Transmission electron micrograph for a fast-aggregated gold colloid cluster (from D A Weitz, private communication).

is removed and the particles aggregate rapidly ($\sim$ 1 sec) or slowly (several weeks) depending on the amount of pyridine added (Creighton 1983). The aggregates may then be concentrated and used for scattering experiments or studied by electron microscopy. Figure 6 illustrates a transmission electron micrograph of one such aggregate cluster, grown via a fast aggregation process. Note the highly ramified structure and the large amount of open spaces, bearing in mind that we are looking at a two dimensional projection of a real three-dimensional object. By analyzing several such electron micrograph pictures, Weitz and Oliveria (1983) were able to show that the number of particles in a cluster scaled as R^D, where R was the cluster size and the fractal dimension D came out to be 1·74 for "fast" aggregates. By digitizing the position of the individual particles, they were also able to calculate the pair correlation function $g(r)$ [see equation (3)] and also arrived at a similar value for D. Neutron scattering measurements have been carried out on a concentrated, precipitated set of aggregates of gold colloid particles in water, using the SANS spectrometer at the University of Missouri Reactor (Sinha *et al* 1985), which utilizes a vertical incident beam. The results for "fast" aggregates, together with light scattering data (appropriately normalized) on this system, are shown as a log-log plot of I vs q in figure 7. Also shown is a curve obtained by least squares fitting of a model based on (7)–(10). Interestingly enough, the r_0 parameter, corresponding to the spherical radius of the particles was fitted by a value of 75 Å, and the fractal dimension D by a value of 1·8, both of which agree extremely well with the values obtained from the electron micrograph analyses, although the statistical averaging available from a scattering experiment is enormously greater. Note that the powerlaw behaviour seen at small q is consistent both with the light-scattering and neutron-scattering data, i.e. no

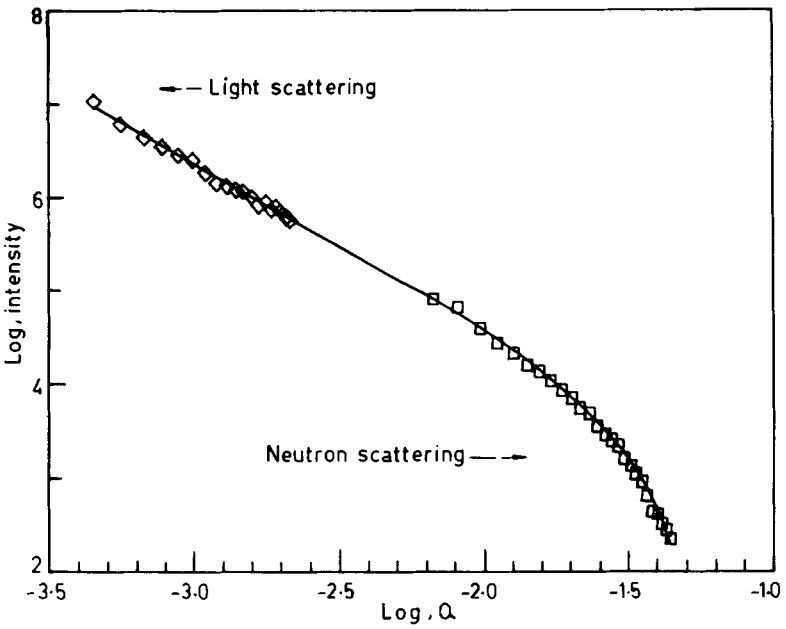

Figure 7. Small angle neutron and light scattering data from "fast" gold colloid aggregates. The light scattering data has been normalized by a suitably chosen scale factor to match smoothly with the SANS data. The solid curve represents a fractal model fit of the kind described in the text, yielding D = 1·802, r_0 = 74·9 Å, ξ = 33,311 Å.

saturation behaviour is seen at small q, implying that the fractal clusters have a size (ξ) of the order of microns or greater.

From results of the kind described in this article, we have a certain degree of confidence in the ability of scattering experiments to confirm and measure the fractal structure of various kinds of objects. Similar experiments, involving light, neutron and x-ray scattering have been used to study the fractal nature of aggregates of silica colloids (Schaefer *et al* 1984), proteins (S H Chen, private communication; Feder 1984), and surface fractal behaviour in porous materials (Bale and Schmidt 1985). Currently, high resolution small angle x-ray scattering experiments are being carried out on synchrotron sources (Dimon *et al* 1985), whereby curves of I vs q spanning the whole q range shown in figure 7 (i.e. from length scales of $\sim$ 50 Å to 10,000 Å) may be obtained at once. Such measurements should, in the near future, be extremely useful in establishing quantitatively the details of fractal structure (and deviations from it) in real materials. The experiments and computer simulations will hopefully be able to establish the way in which fractal dimension depends on the physics of the aggregation process. For instance, $D = 1{\cdot}8$, obtained for the "fast" gold aggregates, is what computer simulations predict for "cluster-cluster" aggregation, i.e. when particles diffuse and join to form clusters which in turn join with other clusters and so on. For the "slow" aggregates, measurements (Dimon *et al* 1985) indicate a higher fractal dimension ($D \sim 2{\cdot}0$), indicating denser clusters.

I should conclude this article, which is dedicated to the memory of Dr Satya Murthy, by expressing my deep appreciation of Dr Satya Murthy's many contributions to the fields of condensed matter physics and neutron scattering (of which the work described here is but a small example) and in particular to its flowering at BARC. I gained much personally and scientifically from my friendship with him, and his tragic and untimely loss is a great blow to the field of neutron scattering.

Acknowledgements

I wish to express my appreciation for the help received from my collaborators in this work, namely J Kjems, T Fretloft, T Witten, D Weitz and J Gethner. Also to the Guggenheim Foundation for a Fellowship during the tenure of which this work was initiated.

References

Aharony A, Gefen Y and Kantor Y 1984 *J. Stat. Phys.* **36** 767

Bale H D and Schmidt P W 1984 *Phys. Rev. Lett.* **53** 596

Creighton J A, Alvarez M S, Weitz D A, Garoff S and Kim M W 1983 *J. Phys. Chem.* **87** 4793

Dimon P, Sinha S K, Weitz D A, Safinya C, Varady W and Smith G 1985 (to be published)

Feder J 1984 *Phys. Rev. Lett.* **53** 1403

Forrest S R and Witten T A 1979 *J. Phys.* **A12** L109

Hausdorff F 1919 *Math. Ann.* **79** 157

Kjems J K, Bauer R, Breiting B, Christensen P, Freltoft T, Jensen L G and Linderholm J 1985 *Proc. Int. Conf. on Neutron scattering in the nineties, Vienna* p. 495

Mandelbrodt B B 1983 *The fractal geometry of nature* (San Franciso: Freeman)

Sander L M 1984 *Kinetics of aggregation and gelation* (eds) F Family and D Landau (New York: North-Holland, Elsevier Science Publishers) p. 13

Schaefer D W, Martin J E, Wiltzius P and Cannell D S 1984 *Phys. Rev. Lett.* **52** 2371
Schafke F W 1968 *Einführung in die Theorie der speziellen Funktionen der mathematischen Physik* (Berlin: Springer) p. 1963
Schmidt P W 1982 *J. Appl. Cryst.* **15** 567
Sierpinski W 1979 *Oeuvres choisies* (eds) S Hartman *et al* (Warsaw: Editions Scientifiques de Pologne)
Sinha S K, Gethner J, Weitz D A and Kaiser H 1985 (to be published)
Turkevitch J, Stevenson P C and Hillier J 1951 *Trans. Faraday Soc.* **11** 55
Von Smoluchowski M 1916 *Phys. Z.* **17** 557
Weitz D A, Huang J S, Lin M Y and Sung J 1984 *Phys. Rev. Lett.* **53** 1157
Weitz D A and Oliveria M 1983 *Phys. Rev. Lett.* **52** 1433
Witten T A and Sander L M 1981 *Phys. Rev. Lett.* **47** 1400
Witten T A and Sander L M 1983 *Phys. Rev.* **B27** 5686